ELSEVIER

www.elsevier.nl/locate/ica

Inorganica Chimica Acta 293 (1999) 1–11

Inorganica Chimica Acta

Preparation and characterisation of new oxovanadium(IV) Schiff base complexes derived from amino acids and aromatic *o*-hydroxyaldehydes

J. Costa Pessoa [a,*], I. Cavaco [a], I. Correia [a], M.T. Duarte [a], R.D. Gillard [b], R.T. Henriques [a], F.J. Higes [c], C. Madeira [a], I. Tomaz [a]

[a] *Centro Química Estrutural, Instituto Superior Técnico, Av. Rovisco Pais, 1049-001 Lisbon, Portugal*
[b] *Department of Chemistry, University of Wales, PO Box 912, Cardiff CF1 3TB, UK*
[c] *Departamento Química Inorgánica, Universidad de Extremadura, 06071 Badajoz, Spain*

Received 19 February 1999; accepted 16 April 1999

Abstract

A range of mostly new oxovanadium(IV) complexes is described. They contain coordinated Schiff bases, made from natural amino acids (glycine, alanine, valine, leucine, isoleucine, methionine, phenylalanine, threonine, aspartic acid, and histidine) and salicylaldehyde or such derivatives as 3-, 4-, or 5-methoxy-salicylaldehyde. The coordination sphere is completed by simple ligands like water, 2,2′-bipyridyl or pyridine. The compounds are characterised and the nature of their coordination spheres shown by analysis, TLC, and by appropriate spectroscopy (EPR, IR, electronic and circular dichroism of solution and solids). In a few cases, magnetic properties are described to establish oxidation state. In several cases, the solubility of the compounds from racemic amino acids differs markedly from those containing the single enantiomer. The crystal and molecular structure of the related (and novel) compound with N-pyridoxylidene-D,L-isoleucinate, [VO(pyr-D,L-Ile)(bipy)]·H_2O is described. It contains two diastereomers. Denoting the chiral vanadium centres as **A** or **C**, these are [**A**(pyr-L-Ile)(bipy)] and [**C**(pyr-D-Ile)(bipy)].

Keywords: Crystal structures; Vanadium complexes; Schiff base complexes

1. Introduction

There have been great efforts in the past few years to find efficient insulin-mimetic vanadium complexes. These would be highly active, easily absorbable and of low toxicity. Well-chosen Schiff base complexes could be suitable candidates. In the context of model systems for reactions of pyridoxal-potentiated enzymes, several studies have concerned the preparation and reactivity of vanadium complexes of N-salicylideneamino acids [1–17], and such ligands are of much current interest in vanadium biocoordination chemistry.

N-salicylideneamino acid vanadium(IV) and (V) complexes often have coordination geometries such as in **I** or **II** [3,5,11,12]. In a few cases, dimeric oxo-bridged compounds **III** have been obtained [4,5,11,13,15]. If bidentate ligands such as bipy or Hhquin (bipy = 2,2′-bipyridine and Hhquin = quinoline-8-ol) are present in the reaction mixture, compounds with structures such as **IV** are normally obtained [3,7,8,13].

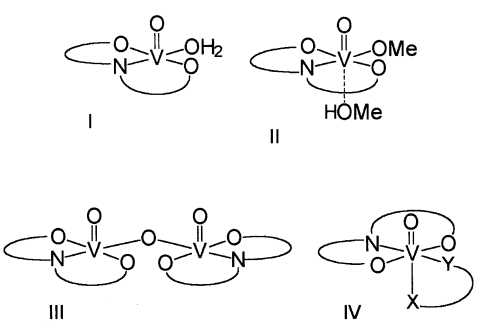

* Corresponding author. Fax: +351-1-846 4455.

0020-1693/99/$ - see front matter
PII: S0020-1693(99)00196-6

The present paper deals with the preparation of several complexes of varying lipophilicity formulated as [VO(dsal–aa)(X)(Y)] containing **V**, a Schiff base ligand resulting from the condensation of an amino acid with salicylaldehyde itself (Hsal) or one of its ring-substituted derivatives denoted here by (Hdsal) **VI**–**IX**, and X = Y = H_2O and/or pyridine; or $\frac{1}{2}$2,2′-bipy. The amino acids are glycine, and natural L-enantiomers of alanine, valine, leucine, isoleucine, methionine, phenylalanine, serine, threonine, aspartic acid and histidine. The complexes were characterised by elemental analysis, IR, EPR, electronic and circular dichroism spectroscopy. In some cases, magnetic moments were measured in the range 4–295 K.

Other than $V^{IV}O$(sal-L-His)$(H_2O)_2$ [14], Na[$V^{IV}V^{V}O_3$-(sal-D,L-Ser)$_2$]·5H_2O [15], [$V^{V}O_3${(dsal(**IX**)-L-Ser)-(H_2O)}$_2$]·2EtOH [4] and [$V^{V}O_2$(naph-L-His)] [18] (dsal(**IX**)-L-Ser = Schiff base formed between o-vanillin (**IX**) and L-serine, and naph = N-2-oxido-1-naphthylmethylene), no vanadium(IV) or (V) complexes with Schiff bases containing amino acids with potentially coordinating side chains have been reported. We report here the preparation of several such complexes containing Schiff bases derived from serine, threonine, aspartic acid and histidine; most are new.

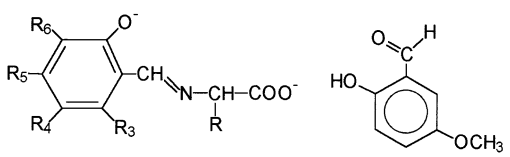

V

VI

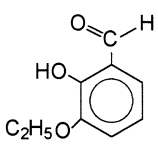

VII

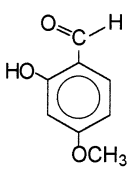

VIII

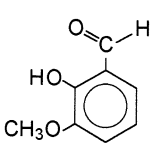

IX

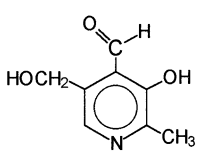

X

The enhanced roles of metal ions in non-enzymatic reactions catalysed by pyridoxal (vitamin B_6-**X**) (e.g. transaminations, racemizations, decarboxylations, β-eliminations) have been extensively studied [19–22]; an intermediate Schiff base complex is expected to form. Because of the inherent reactivity of the system, or the difficulty in obtaining good crystals and maintaining them during X-ray data collection, few complexes have been structurally characterised. However, oxovanadium(IV/V) is one of the most active metal ions in β-eliminations and several of its N-salicylidene- and N-naphthalideneamino acidato complexes have been characterised by X-ray diffraction [3,5,8–13]. This work includes the first preparation and X-ray characterisation of an oxovanadium N-pyridoxylideneamino acidato complex, [VO(pyr-D,L-Ile)(bipy)]·H_2O.

2. Experimental

2.1. Synthesis of complexes

The complexes [$V^{IV}O$(dsal–aa)(H_2O)] (dsal–aa = **V**, dsal = **VI**–**IX**) were obtained as described previously [3,5,17] for similar N-salicylideneamino acidato compounds. Complexes formulated as [$V^{IV}O$(dsal–aa)(bipy)] were obtained by methods similar to that employed for [$V^{IV}O$(sal-L-Ala)(bipy)] [3]. Compounds formulated as V_2O_3(dsal(**IX**)-L-Met)$_2$(py)$(H_2O)_2$ and V_2O_3(dsal(**IX**)-L-Val)$_2$(py)$(H_2O)_2$ (described later) were prepared by a procedure similar to that for [$V^{IV}O$(sal-Gly)$(py)_2$]·H_2O [3,5], i.e. by dissolving [$V^{IV}O$(dsal(**IX**)-L-Met)(H_2O)] or [$V^{IV}O$(dsal(**IX**)-L-Val)(H_2O)], respectively, in pyridine/water. In other similar preparations with salicylaldehyde derivatives **VI**–**IX** and/or with other amino acids, no precipitation normally occurred. In a few cases, no simple formulation was compatible with the elemental analysis. Table 1 summarises those solids: compounds **1**–**31** obtained by these routes which had good elemental analyses.

Also listed in Table 1 is complex **32**. This complex can be prepared from H_2O/MeOH (or /EtOH) solutions containing $VOSO_4$, D,L-isoleucine, pyridoxal·HCl and bipy in 0.9:1:1:1 molar ratio. Depending on the concentration, precipitation started after times from a few minutes to several days. If the solutions were too dilute, no precipitation occurred.

2.2. TLC experiments

Most preparations were monitored by TLC, on Merck TLC plates (Art. 5626, 10 × 20 cm). Samples of 1–3 μl of the reaction mixture were applied to the plates 20 mm from the bottom. Elutions were carried out in Camag twin chambers with walls covered with filter paper impregnated with the eluent. Eluents used were (**A**) ethanol/water (7:3), (**B**) n-butanol/ethanol/propionic acid/water (10:10:2:5). When the eluents reached approximately 120 mm from the bottom, the

Table 1
Formulation proposed for the complexes isolated and elemental analyses: experimental (and theoretical)

Compounds	Elemental analyses			
	% C	% H	% N	% S, Na or V
[VO(dsal(**VII**)-Gly)(H_2O)]·2H_2O (**1**)	38.9 (38.61)	4.9 (5.01)	4.0 (4.09)	
[VO(dsal(**IX**)-Gly)(bipy)]·H_2O (**2**)	54.0 (53.58)	4.0 (4.27)	9.3 (9.37)	
[VO(dsal(**VII**)-Gly)(bipy)]·$\frac{1}{2}H_2O$ (**3**)	56.8 (55.88)	4.3 (4.02)	9.3 (9.31)	
[VO(dsal(**VII**)-Ala)(bipy)] (**4**)	57.2 (57.65)	4.5 (4.62)	9.0 (9.17)	
[VO(dsal(**IX**)-Ala)(bipy)]·H_2O (**5**)	54.1 (54.55)	4.4 (4.58)	8.8 (9.09)	
[VO(dsal(**VII**)-Val)(H_2O)] (**6**)	48.0 (48.28)	5.5 (5.49)	3.9 (4.02)	
[VO(dsal(**IX**)-Val)(H_2O)]·$\frac{1}{2}H_2O$ (**7**)	45.6 (45.49)	5.0 (5.29)	4.0 (4.08)	**V**: 14.0 (14.8)
[VO(dsal(**IX**)-Val)(bipy)]·H_2O (**8**)	58.3 (58.37)	4.9 (4.90)	8.7 (8.17)	**V**: 10.3 (10.2)
VO(dsal(**IX**)-Val)(H_2O)·$\frac{1}{2}$py·$\frac{1}{2}H_2O$ (**9**)	48.8 (48.64)	5.2 (5.40)	5.4 (5.49)	
[V_2O_3(dsal(**IX**)-Val)(py)(H_2O)$_2$]	(48.76)	(5.15)	(5.50)	
[VO(dsal(**VII**)-Val)(bipy)] (**10**)	59.3 (59.26)	5.2 (5.18)	8.5 (8.64)	
[VO(dsal(**VI**)-Ile)(bipy)]·$\frac{1}{2}H_2O$ (**11**)	58.2 (58.18)	5.2 (5.29)	8.3 (8.48)	
[VO(dsal(**VII**)-Ile)(H_2O)]·H_2O (**12**)	47.5 (47.38)	6.1 (6.10)	3.6 (3.68)	
[VO(dsal(**VIII**)-D,L-Ile)(H_2O)] (**13**)	48.4 (48.29)	5.5 (5.50)	4.0 (4.02)	
[VO(dsal(**VIII**)-Ile)(bipy)]·H_2O (**14**)	57.4 (57.15)	5.3 (5.39)	8.3 (8.33)	
[VO(dsal(**IX**)-Ile)(H_2O)]·H_2O (**15**)	46.2 (45.91)	6.1 (5.78)	3.4 (3.82)	**V**: 13.5 (13.9)
[VO(dsal(**IX**)-Leu)(bipy)]·$\frac{1}{2}H_2O$ (**16**)	58.2 (58.18)	5.2 (5.29)	8.4 (8.48)	
[VO(dsal(**VII**)-Met)(bipy)]·3/2H_2O (**17**)	52.7 (52.84)	5.1 (5.17)	7.5 (7.70)	**S**: 5.8 (5.88)
[VO(dsal(**IX**)-Met)(bipy)]·2H_2O (**18**)	50.5 (51.11)	4.9 (5.03)	7.5 (7.77)	**S**: 5.9 (5.93)
VO(dsal(**IX**)-Met)(H_2O)·$\frac{1}{2}$ py·$\frac{1}{2}H_2O$ (**19**)	45.1 (44.88)	4.8 (4.98)	5.0 (5.06)	**S**: 7.8 (7.73)
[V_2O_3(dsal(**IX**)-Met)(py)(H_2O)$_2$]	(44.98)	(4.75)	(5.08)	(7.75)
[VO(dsal(**IX**)-Phe)(H_2O)] (**20**)	53.4 (53.27)	4.6 (4.73)	3.6 (3.65)	
[VO(dsal(**IX**)-Phe)(bipy)]·H_2O (**21**)	60.1 (60.12)	4.5 (4.86)	7.4 (7.79)	
[VO(dsal(**VII**)-phe)(bipy)] (**22**)	54.1 (54.56)	4.8 (4.83)	3.5 (3.53)	
[VO(sal-Ser)(bipy)]·H_2O (**23**)	53.5 (53.58)	4.1 (4.27)	9.2 (9.37)	**Na**: 0.08 (0.0)
Na[V_2O_3(sal-Ser)$_2$]·5H_2O (**24**)	36.9 (35.47)	4.0 (4.17)	4.1 (4.14)	**Na**: 3.2 (3.39)
[VO(dsal(**IX**)-Ser)(bipy)]·H_2O (**25**)	52.5 (52.73)	4.3 (4.42)	8.6 (8.78)	
[VO(dsal(**VII**)-Thr)(bipy)] (**26**)	56.6 (56.56)	4.7 (4.75)	8.6 (8.62)	
[VO(sal-Thr)(bipy)]·3/2H_2O (**27**)	54.1 (53.51)	4.4 (4.70)	8.7 (8.92)	**Na**: 0.14 (0.0)
Na[VO(sal-Asp)] (**28**)	40.6 (40.76)	2.5 (2.49)	4.3 (4.32)	**Na**: 6.2 (7.1), **V**: 14.7 (15.7)
Na[VO(sal-Asp)(H_2O)]	(38.62)	(2.95)	(4.09)	**Na**: (6.7), **V**: (14.8)
Na_2[V_2O_3(sal-Asp)$_2$]	(39.78)	(2.43)	(4.22)	**Na**: (6.9), **V**: (15.3)
[VO(sal-His)(H_2O)]·$\frac{1}{2}H_2O$ (?) (**29**)	44.3 (44.46)	3.7 (4.02)	11.1 (11.96)	**Na**: 0.1 (0.0), **V**: 13.8 (14.5)
[VO(sal-His)(bipy)]·3.5H_2O (?) (**30**)	49.6 (50.84)	4.0 (4.82)	12.5 (12.89)	**Na**: 0.1 (0.0), **V**: 10.0 (9.4)
[VO(dsal(**VII**)-His)(H_2O)] (?) (**31**)	48.9 (46.64)	4.5 (4.44)	10.9 (10.88)	
[VO(pyr-D,L-Ile)(bipy)]·H_2O (**32**)	56.0 (55.49)	5.8 (5.43)	10.7 (10.98)	

plates were removed and dried. The chromatogram was developed with ninhydrin–collidine–copper solution prepared according to Moffat and Lytle [23]. Distinct and clear spots (S) corresponding to the Schiff base complexes are normally detected. Distinct spots (AA) are also detected at the R_f of the free amino acids and the spots S each tailed to the spot AA. This is due to hydrolysis of the Schiff base during elution. R_f values are greater for [VO(dsal–aa)(Z)] complexes (Z = H_2O, ethanol or butanol from the eluent) than for the [VO-(dsal–aa)(bipy)] compounds, and also higher with eluent **A** than with **B**.

In several instances, preparative mixtures of the generally appropriate composition yielded no solid. Among such solutions, there were a number where distinct spots were detected at R_f values corresponding to the desired Schiff base complex. This was particularly the case for derivatives of L-amino acids, conceivably reflecting the formation but failure to precipitate of these usually more soluble optically active compounds. The observed spots included: [VO(sal-L-Glu)(Z)] (R_f = 0.54 (**A**) and 0.53 (**B**)) and [VO(sal-L-Glu)(bipy)] (R_f = 0.49 (**A**) and 0.49 (**B**)), [VO(sal-L-Ser)(Z)] (R_f = 0.71 (**A**) and 0.62 (**B**)) and [VO(sal-L-Thr)(Z)] (R_f = 0.73 (**A**) and 0.62 (**B**)), [VO(sal-L-Asp)(Z)] (R_f = 0.61 (**A**) and 0.49 (**B**) and other spots), [VO(sal-L-Asp)(bipy)] (R_f = 0.60 (**A**) and 0.50 (**B**) and other spots), [VO(sal-L-Arg)(Z)] (R_f = 0.64 (**A**) and 0.48 (**B**)) and [VO(sal-L-Arg)(bipy)] (R_f = 0.41 (**A**) and 0.37 (**B**)).

2.3. Magnetic measurements

The magnetic susceptibilities were measured for compounds **9**, **23** and **28** in the range 4–298 K using a 7-Tesla Oxford Instruments Faraday system coupled to a Sartorius S3D-V microbalance, operating at 1 Tesla.

2.4. Spectroscopic measurements

The circular dichroism spectra were run on a Jasco 720 spectropolarimeter either with the 175–700 nm or with the red sensitive (400–1000 nm) photomultipliers, isotropic absorption spectra with a Perkin–Elmer λ9 spectrophotometer and electron spin resonance spectra on a Bruker ER 200d (connected to a Brucker B-MN C5) spectrometer.

2.4.1. CD spectra of solid complexes

Samples were prepared as described previously [3] and placed between two microscope slides. One to three of such paired microscope slides were placed in the sample compartment. Each final spectrum is the average of four to six spectra in all, recorded as described in [3].

2.4.2. Solution absorption and CD spectra

These were recorded for solutions of the complexes in methanol and $CHCl_3$ (except for complexes **23**–**31**, which were only in methanol). Before preparing the solutions, oxygen was removed from the solvents by bubbling N_2. All spectra were recorded immediately after the preparation of the solutions: the cells had their stoppers reinforced with Parafilm strips but no special care was taken to remove oxygen from the cell space above the solutions. CD and absorption spectra in the visible range were recorded with concentrations in the range $(2–6) \times 10^{-3}$ M. In the UV range, solutions with concentrations in the range $(2–5) \times 10^{-4}$ M were first prepared and spectra measured; CD and absorption spectra were again run after a 1:10 dilution.

2.5. Crystal structure determination of [VO(pyr-D,L-Ile)-(bipy)]·H_2O (32)

Crystal data, data collection and refinement details for [VO(pyr-D,L-Ile)(bipy)]·H_2O are given in Table 2. Cell dimensions were determined from the measured θ values for 25 intense reflections with $10 < \theta < 12°$. Examination of three standard reflections showed no sign of crystal deterioration. The data were corrected for Lorentz and polarization effects, and were also corrected for absorption effects using an empirical method based on azimuthal scan data. The structure was solved by direct methods and subsequent Fourier differences and refined by full-matrix least-squares using anisotropic thermal parameters for non-hydrogen atoms. Hydrogen atoms were inserted in idealised positions and allowed to ride on the parent C and O atoms. Hydrogen atoms from the water molecule were found in the difference map and refined with restraints. SHELXS-86 and SHELX-97 were used for structure solution and for refinement, respectively.

3. Results and discussion

For most of the compounds in Table 1, the elemental analyses are compatible with those expected. Substituents –OMe and –OEt in **V** induce no steric constraints or inductive effects which might significantly affect the stability or reactivity relative to the parent salicylaldehyde derivatives.

3.1. IR spectra

All complexes present a broad band due to water centred at approximately 3400 cm^{-1}, less pronounced but also clear in complexes where H_2O is not included in their formulation. A medium/strong band at 1530–1560 cm^{-1}, always present, may originate from the vibration of the (Ph–)C–C(=N) bond [24] and typifies

Table 2
Crystal data, data collection and refinement details for [VO(pyr-D,L-Ile)(bipy)]·H_2O

Crystal data	
Formula	$C_{24}H_{24}N_4O_6V$
Formula weight	515.4
Crystal system	monoclinic
Space group	$P2_1/n$
a (Å)	12.464(3)
b (Å)	15.347(4)
c (Å)	12.868(3)
β (°)	99.10(2)
V (Å^3)	2430.5(10)
Z	4
F(000)	1068
D_{calc} (g cm^{-3})	1.409
Crystal size (mm)	$0.65 \times 0.22 \times 0.20$
Data collection instrument	Enraf–Nonius CAD4
Radiation monochromated (Å)	Mo Kα, $\lambda = 0.71073$
Temperature (°C)	25
2θ Range (°)	2.08–24.98
Scan type	ω–2θ
Index ranges	$-14 \le h \le 14$, $-18 \le k \le 2$, $-2 \le l \le 15$
Reflections collected	6138
Independent reflections	4270 [$R_{int} = 11.02\%$]
Observed reflections	2540 [$F_o > 4\sigma(F_o)$]
Refinement method	full-matrix least-squares on F^2
Number of refined parameters	306
Absorption coefficient (mm^{-1})	0.455
Final R indices (observed data) (%)	$R_1 = 12.31$, $wR_2 = 18.08$
w	$1/[\sigma^2(F_o) + 0.0348P^2 + 16.76P]$ where $P = \{\max(F_o^2) + 2F_c^2\}/3$
Goodness-of-fit	1.037
Data/restraints/parameters	4270/3/314
Largest difference peak and hole (e Å^{-3})	0.458 and −0.347 (near the vanadium atom)

complexes derived from salicylaldehyde [3,5,24,25]. All complexes present very strong and broad bands corresponding to ν(C=N) and ν_{as}(COO) centred around 1630–1660 cm^{-1}. The bands are probably broadened because of overlap with aromatic ring-carbon stretching. In some cases, peaks at approximately 1620–1660 and 1585–1605 cm^{-1} emerge from the broad background band corresponding to ν(C=N) and ν_{as}(COO), respectively. The symmetric carboxylate stretch, ν_s(COO), probably corresponds to the medium/strong bands in the range 1325–1380 cm^{-1}, though in some cases, this range is confusingly crowded. The large difference between ν_{as}(COO) and ν_s(COO) indicates a monodentate coordination of this group [26]. Medium to strong bands in the range 1290–1320 cm^{-1} probably correspond to ν(O–Ph). The ν(V=O) band appears in the range 950–995 cm^{-1}.

Beside these general features, some groups of complexes manifest others more clearly, e.g. in those containing 2,2′-bipy, weak bands at 3020–80 cm^{-1}, due to aromatic C–H stretch, and, in complexes involving Val, Leu, Ile and Met, medium bands in the range 2840–2980 cm^{-1} due to the methyl C–H stretch.

3.2. ESR spectra

The ESR spectra may help to elucidate which groups coordinate in equatorial position in solution. The spin Hamiltonian parameters were calculated either following the method described in [27] by an iterative procedure using the corrected equations given in [14], or by simulation of spectra using the program EPRPOW[1]. The $g_{\parallel}$, $A_{\parallel}$, $g_{\perp}$ and $A_{\perp}$ values obtained for all complexes formulated as [VO(dsal–aa)(H_2O)] are in the ranges: 1.935–1.950, 1.980–1.985, 167–170 $\times 10^{-4}$ cm^{-1} and 62–64 $\times 10^{-4}$ cm^{-1}, respectively, and those for all [VO(dsal–aa)(bipy)] in the ranges: 1.939–1.954, 1.975–1.985, 161–166 $\times 10^{-4}$ cm^{-1} and 57–62 $\times 10^{-4}$ cm^{-1}, respectively. These results are as expected for the present ligand donor atoms [3,5,27], with the structures found for [VO(sal-L-Ala)(H_2O)] [3,10] and [VO(sal-L-Ala)(bipy)] [3]. The presence of 2,2′-bipy slightly decreases $A_{\parallel}$ and increases $g_{\parallel}$.

3.3. CD and absorption spectra

3.3.1. Visible range

In the visible isotropic absorption spectra, band I ($d_{xy} \rightarrow d_{xz},d_{yz}$) normally appears broad, between approximately 650 and 900 nm (at least), and in some cases is hardly distinct from the tail of bands at lower wavelengths (e.g. for complexes **7**, **9**, **18** and **22**). A band at 540 ± 20 nm is apparently common to all complexes. However, while for some a distinct maximum appears (e.g. for **19** and [VO(sal-L-Ala)(H_2O)] [3] in methanol, or **19** and **20** in $CHCl_3$), this band often appears as a shoulder on higher intensity bands from the UV (e.g. for **7**, **9**, **18**, **20**, **22** in methanol, and **9**, **5**, **22** in $CHCl_3$): in a very few cases not even such a shoulder is apparent (e.g. for **5** in methanol and **8** in $CHCl_3$). This shoulder probably corresponds to band II ($d_{xy} \rightarrow d_{x^2-y^2}$).

In the visible, circular dichroism generally gives more useful structural information on oxovanadium(IV) complexes than absorption spectra [3,5,28]. That is so here too. For the complexes formulated [VO(dsal-L-aa)(bipy)], the CD spectra in methanol and $CHCl_3$ were similar (although the $\Delta\varepsilon_m$ and λ_{max} are unequal). For compounds formulated [VO(dsal-L-aa)(H_2O)], differences were normally found between the CD spectra in the two solvents. In some cases, these differences were small; in other cases, they may be attributed to changes in $\Delta\varepsilon_m$ and λ_{max} of the bands (e.g. for **7**). Remarkably bands may apparently sign change (e.g. for **20**, in methanol, where V^{IV} oxidizes easily to V^{V} and strong positive bands appear at $\lambda < 700$ nm). These subtle spectroscopic changes in electronic absorptions are not reflected in the isotropic absorption spectra discussed later. For **20**, and very likely also for **7**, these chiroptical changes may mean either that the integrity of the compound or vanadium oxidation state in solution is not preserved or that the structural factors that dominate the CD signal alter drastically.

Fig. 1 includes CD spectra of methanolic solutions of complexes containing L-valine. For these and almost all the [VO(dsal-L-aa)(X)] (X = H_2O, 2,2′-bipy) complexes prepared, the CD spectra show, in the range 630–900 nm, two clear bands ($d_{xy} \rightarrow d_{xz},d_{yz}$): Ia (at longer wavelengths), $\Delta A < 0$; Ib, $\Delta A > 0$, emphasising the non-sym-

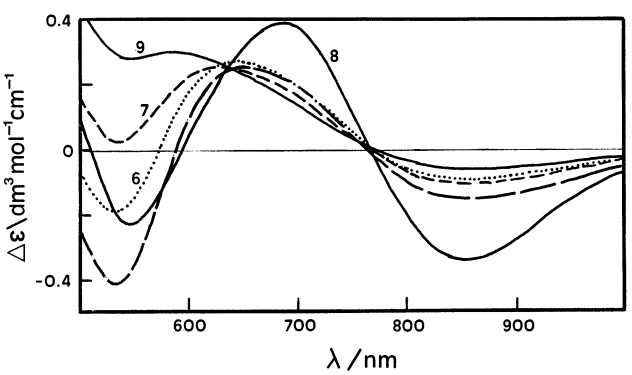

Fig. 1. Circular dichroism spectra of methanolic solutions of several Schiff base complexes containing L-valine ($\approx$3–5 mmol dm^{-3}): [VO(sal-L-Ala)(H_2O)] (dashed line), **6** (dotted line), **7** (broken line), **8** (unbroken line), **9** (unbroken line).

[1] EPRPOW, developed by L.K. White, R.L. Belford (University of Illinois) and modified by L.K. White, N.F. Albanese, N.D. Chasteen (University of New Hampshire) to include both Lorentzian and Gaussian line shape functions, an $I = 7/2$ nucleus, a 4th hyperfine interaction and multiple sites having different linewidths (1978).

metrical nature of the ligand field, and band II ($d_{xy} \rightarrow d_{x^2-y^2}$, $\Delta A < 0$) in the range 520–570 nm. The coordination geometry is, then, similar in all cases. The pattern $-,+,-$ for II, Ib, and Ia, respectively, is identical to that for the corresponding salicylaldehyde complexes [3,5] also indicating similar coordination geometry; the CD pattern for [VO(dsal(**IX**)-L-Val)(bipy)] (**8**) is the same as for other complexes formulated as [VO(dsal-L-aa)(H_2O)] but the λ_{max} differ. Comparing the present complexes [VO(dsal-L-aa)(bipy)], and those of Refs. [3,5] with the corresponding [VO(dsal-L-aa)(H_2O)], band Ia shifts to the UV by approximately 20–60 nm; band Ib shifts to the red by approximately 20–50 nm and band II by approximately 10–30 nm.

Fig. 2 shows the CD spectra of the same valine-containing complexes dispersed in KBr disks. Such spectra have ill-defined base lines, but band Ia, with $\lambda_{max} \approx 920 \pm 20$ nm, certainly has a negative Cotton effect in all complexes including **6**, **7** and **9**. For most complexes (except **20**) the pattern of the CD spectra in the solid state and in solution are the same, so the coordination geometry does not change upon dissolution. The small differences observed between phases result from relatively small changes in the λ_{max} and relative $\Delta\varepsilon_m$ values of the bands in both types of spectra.

3.3.2. UV range

In isotropic absorption, [VO(dsal-L-aa)(X)] and those formulated as containing a V_2O_3 core normally have bands at 230–240 nm with $\varepsilon = (10–15) \times 10^4$ and 290–300 nm with $\varepsilon = (4–10) \times 10^3$ dm^3 mol^{-1} cm^{-1}, the complexes containing bipy or py corresponding to the higher range of the ε values. The bands at higher energy are probably associated with benzene ring $\pi \rightarrow \pi^*$ [29] and charge transfer [30] transitions. Similar bands occur in [VO(sal-L-aa)(X)] (sal-L-aa = N-salicylidene-L-amino acidate with non-coordinating side chain, X = H_2O, py or bipy) [3,5]. The imine band (see below) normally appears at 380 ± 5 nm (X = H_2O, **9** and **19**) or 390 ± 10 nm (X = bipy), with ε values in the range 1400–1800 dm^3 mol^{-1} cm^{-1}. Although the extinction coefficients show some differences between MeOH and $CHCl_3$ solutions, the biggest difference in λ_{max} is only 10 nm.

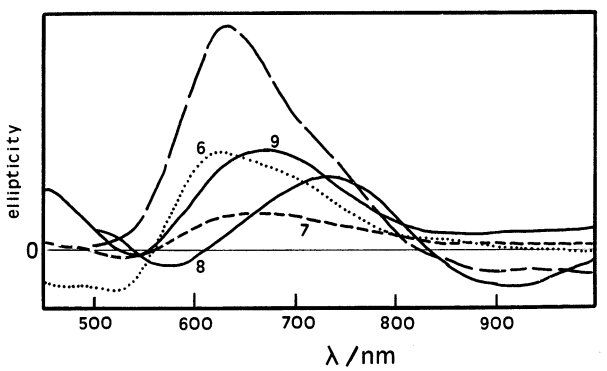

Fig. 2. Circular dichroism spectra of several Schiff base complexes dispersed in KBr disks: [VO(sal-L-Ala)(H_2O)] (dashed line), **6** (dotted line), **7** (broken line), **8** (unbroken line), **9** (unbroken line).

As in the visible, the CD spectra in the UV range are more informative than the corresponding absorption spectra. Overall, for the complexes [VO(dsal-L-aa)(X)] (X = H_2O, bipy) the sign pattern of the Cotton effects associated with the UV absorption bands is constant within the two series and this certainly reflects the fact that the main stereochemical factors that determine the Cotton effect are the same in most complexes.

In methanolic solutions, complexes [VO(sal-L-aa)(H_2O)] possess [3,5] a low-energy absorption band around 374 ± 2 nm (CD and absorption), attributed to a $\pi \rightarrow \pi^*$ transition originating mainly in the azomethine chromophore. These bands display negative Cotton effects as found for the related zinc [25], copper [31], and cobalt(II) [29] chelates. For the present series of $V^{IV}O$ chelates of similar Schiff bases either in MeOH or $CHCl_3$, this intense CD band appears in a similar range: 380 ± 5 nm. Also, as for complexes derived from salicylaldehyde [3,5] the imine CD bands are flanked by a shoulder at 330–350 and a band at 300–330 nm, normally also negative, and a positive band at 270–290 nm. The relative λ_{max} of these bands determines the possibility of clearly distinguishing them.

CD spectra of the [VO(dsal-L-aa)(bipy)] complexes are similar but with red shifts by approximately 10–20 nm (imine band) and approximately 20–30 nm (shoulder). Because of the very high absorption for $\lambda < 280$ nm, the CD spectra are very noisy.

3.4. Magnetic data

Magnetic susceptibilities for complexes **9** and **23** are shown in Fig. 3. For **23** the curve $\chi_p \times T$ versus T shows a maximum at approximately 12 K indicating weak ferromagnetic interaction at low temperatures. The magnetic susceptibility results, after correction for the corresponding χ_d, were fitted to a Curie–Weiss law $\chi_p = C/(T - \theta) + \text{TIP}$ yielding the values indicated in Table 3. For **23** and **28** the results are compatible with the presence of oxovanadium(IV) complexes with no significant antiferromagnetic interactions.

3.5. Specific dsal–aa complexes

Having discussed general features, we now discuss specific cases, particularly compounds **9**, **19** and those containing amino acids with potentially coordinating side chains.

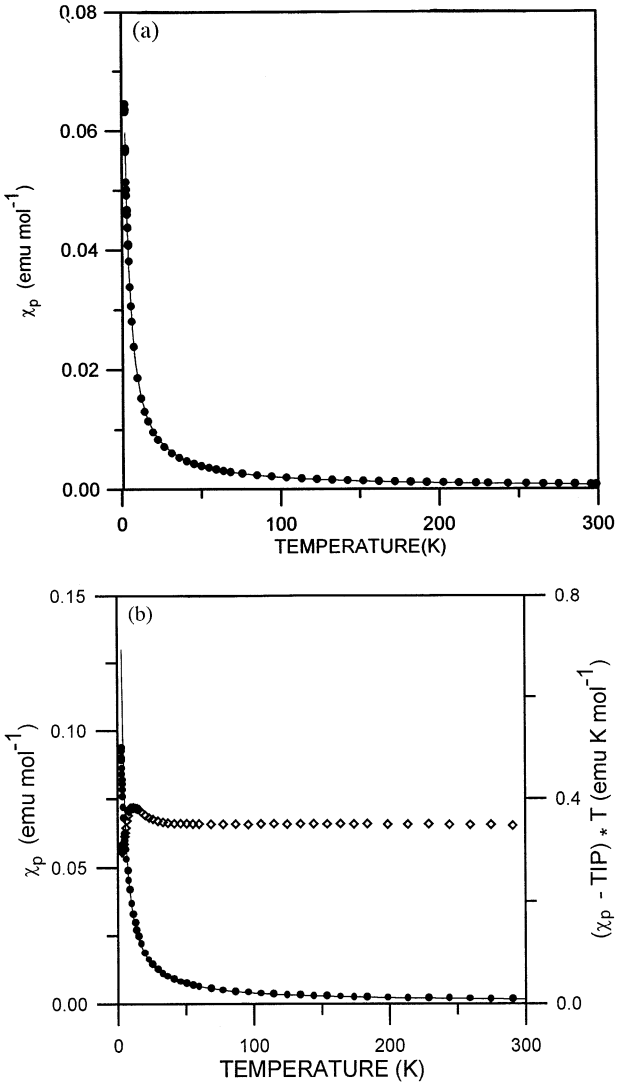

Fig. 3. Temperature dependence of the magnetic susceptibilities (circles, left scale) of compounds **9** (a) and **23** (b), in the range 4–298 K with the full lines corresponding to the best data fits. In (b) the curve $(\chi_p - \mathrm{TIP}) \times T$ vs. T is also included (squares, right scale).

3.5.1. Compounds *9* and *19*

The magnetic susceptibilities χ_p of **9** (Fig. 3) indicate a paramagnetic behaviour, i.e. the complex is not a $V^{IV}O$ dimer. From the Curie constant C, assuming $g_{av} = 2.0$, the amount of species with $S = 1/2$ is calculated as 53.3%; this indicates a complex with a formulation involving 50% V^{V} and 50% V^{IV}. Therefore we suggest for solid **9** the formulation V_2O_3(dsal(**IX**)-Val)$_2$(py)$(H_2O)_2$, i.e. a mixed valence dimer with coordination geometry such as **III** containing a $V^{IV}V^{V}O_3^{3+}$ unit with pyridine either equatorial or axial. For **19** we suggest a similar formulation and structure.

The CD spectra (UV range) of **9** in methanol and $CHCl_3$ differ: in $CHCl_3$, 320 nm ($\Delta\varepsilon = -2.5$ dm^3 mol^{-1} cm^{-1}), 358 nm ($\Delta\varepsilon = -2.6$), and 390 nm (sh, $\Delta\varepsilon = -2.0$) but, in methanol, 312 nm ($\Delta\varepsilon = -2.65$), and 388 nm (sh, $\Delta\varepsilon = +0.087$). In both solvents, the relative intensities of the bands differ from those for [VO(dsal-L-aa)(X)] (X = H_2O, bipy). Compound **19** shows a similar property. Its spectrum in $CHCl_3$ resembles those for complexes of monomeric Schiff bases: 315 nm ($\Delta\varepsilon \approx -2.4$ dm^3 mol^{-1} cm^{-1}), 360 nm (sh, $\Delta\varepsilon = -3.0$), 387 nm ($\Delta\varepsilon = -3.8$) and 470 nm ($\Delta\varepsilon = +0.35$) but in methanol the spectrum looks totally different, although the maximal wavelengths do not in fact differ much: 308 nm ($\Delta\varepsilon = -4.45$ dm^3 mol^{-1} cm^{-1}), 340 nm ($\Delta\varepsilon = -2.6$), 385 nm ($\Delta\varepsilon = -1.5$) and 455 nm ($\Delta\varepsilon = +0.55$).

For compounds **9** and **19**, bands Ia and Ib in the solution and solid CD spectra are very similar (cf. Figs. 1 and 2); in the region of band II, the CD spectrum of the solid is too noisy for safe comparison. The CD spectrum (visible range) of **9** (Fig. 1) with its different structure certainly differs from the spectra of **6**–**8** and of [VO(sal-L-Val)(H_2O)] [5]. This CD spectrum is also compatible with formulation as a mixed-valence complex containing a $V^{IV}V^{V}O_3^{3+}$ unit: bands Ia and Ib (due to the V^{IV} half unit) are clear, and the increased intensity for $\lambda < 600$ nm is probably due to a l.m.c.t. of type p(phenolate oxygen) $\rightarrow d$(vanadium) [32] with λ_{max} at 400–450 nm (due to the V^{V} half unit).

3.5.2. Serine and threonine complexes

Only complexes **23**–**27** could be characterised as solids, but there is good evidence for the formation and existence of several analogues in solution. Typically, mixtures containing VO^{2+}, Hsal and L-Ser or L-Thr form [V^{IV}O(sal-L-Ser)(Z)] and [V^{IV}O(sal-L-Thr)(Z)] (Z = H_2O, EtOH or MeOH). This was confirmed by TLC, CD and ESR spectra. These species are quite stable; in TLC, pinkish spots were detected for [V^{IV}O(sal-L-Ser)(Z)] ($R_f = 0.71$ (eluent **A** of Section 2) and 0.62 (eluent **B**)) and yellowish spots for [V^{IV}O(sal-

Table 3
Values of C (Curie constant), TIP (temperature independent paramagnetism) and θ (Weiss constant) obtained by fitting the magnetic susceptibility results to the Curie–Weiss law [a]: $\chi_p = C/(T-\theta) + \mathrm{TIP}$, and calculations of g or μ_{eff} from the equation for the Curie constant C [$C = (g^2\mu^2 S(S+1)N)/(3K)$]

Compound no.	**9**	**23** [d]	**28**
C (emu K mol^{-1})	0.196	0.350	0.391
TIP (emu mol^{-1})	5.5×10^{-5}	4.52×10^{-4}	2.91×10^{-4}
θ (K)	−0.3	0.3	−1.3
g [b]	1.449	1.93	2.04
μ_{eff} [c]	1.25	1.67	1.77
χ_d (emu mol^{-1})	-2.05×10^{-4}	-2.45×10^{-4}	-1.4×10^{-4}

[a] The fitting parameters (r^2) were always greater than 0.999.
[b] Value of g calculated from the Curie constant C, assuming $\mu_{eff} = 1.73$ BM.
[c] Value of μ_{eff} calculated from the Curie constant C, assuming $g = 2.0$.
[d] Data fitted for $T > 40$ K.

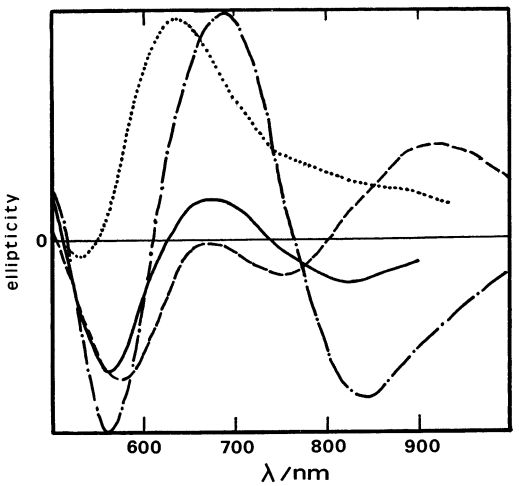

Fig. 4. Circular dichroism spectra of Schiff base complexes (≈ 3–5 mmol dm^{-3}): [VO(sal-L-Ala)(bipy)] (unbroken line), **23** (broken line), **27** (dots and dashes), and **29** (dotted line) dispersed in Nujol mulls.

L-Thr)(Z)] ($R_f = 0.73$ (A) and 0.62 (B)). Despite this, no solid was isolated except **24** which shows no optical activity at least in the range $400 < \lambda < 1000$ nm. Based on the elemental analysis (including Na, Table 1) and on the fact that its IR coincides with the IR of crystals of $Na[V_2O_3(sal\text{-}D,L\text{-}ser)_2]\cdot 5H_2O$ [15], we conclude this is the correct formulation for **24**. Amino acid racemization in these systems is not uncommon and has been followed by HPLC for the system VO^{2+}, Hsal and L-Asn [33]. The single crystal X-ray characterisation of $[V^VO_3\{(dsal(\mathbf{IX})\text{-L-Ser})(H_2O)\}_2]\cdot 2EtOH$, isolated from similar solutions on standing for several weeks, does not prove that racemization of the amino acid has not occurred. In fact spontaneous resolution may lead to the separate formation of crystals of $[V^VO_3\{(dsal(\mathbf{IX})\text{-L-Ser})(H_2O)\}_2]\cdot 2EtOH$ and of $[V^VO_3\{(dsal(\mathbf{IX})\text{-D-Ser})(H_2O)\}_2]\cdot 2EtOH$, and it may be the case that only one type was studied by X-ray diffraction.

On ageing solutions containing VO^{2+}, Hsal and L-Thr, crystals of $(NH_4)_4(Na)_2[V_{10}O_{28}]\cdot 10H_2O$ were obtained after 3–4 weeks. These were characterised by X-ray diffraction and are identical with those from similar solutions (but containing glycylglycine [16]). Therefore, in this system with L-Thr, metal ion oxidation and deamination of the amino acid also yields NH_4^+, identified as a counter ion of the decavanadate.

The elemental analysis for **23** and **25**–**27** are good, and their IR and ESR agree with their formulation and with a coordination geometry such as **IV**. The magnetic susceptibilities for **23** also agrees with a monomeric formulation for this compound (see above).

CD spectra of **23**, **27** and $[V^{IV}O(sal\text{-L-Ala})(bipy)]$ [3] dispersed in Nujol mulls are in Fig. 4. The CD signal of band I for **23** is abnormal. It is low and quite noisy so may be an artifact; if genuine, it may result from a different proportion of diastereomers **XIa** and **XIb** [3,5,12,34,35] in **23** as compared with other complexes.

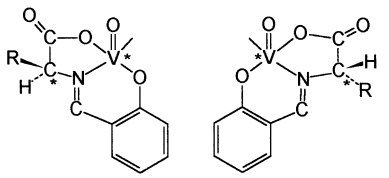

XIa XIb

3.5.3. Aspartic acid complexes

Several solids were obtained from solutions containing VO^{2+}, Hsal and L-Asp and, in some cases, 2,2′-bipy. In solutions containing 2,2′-bipy, a brownish orange solid separated after 2 h. Its elemental analysis closely fits the formulation $[V^{IV}O(sal\text{-Asp})(bipy)]\cdot EtOH\cdot 3/2H_2O$. From mixtures containing no 2,2′-bipy, precipitation of bluish solids started only after several days. From one experiment, **28** was isolated after 1 week. In a different batch, a solid separated after 6 weeks which analysed for $NaV_4O_8(sal\text{-Asp})$.

The IR spectrum of complex **28** is compatible with the coordination of a sal-Asp ligand to VO^{2+}, including bands at 1660 ($\nu_{C=N}$), a strong peak at 1640, a very intense band at 1580 (ν_{COO^-}), the peak at 1550 typical of N-salicylideneamino acidato ligands and $\nu_{V=O}$ at 950 cm^{-1}. In the ESR of **28** in H_2O:ethyleneglycol (2:1), only one complex is present with spin-Hamiltonian parameters: $g_{\|} = 1.943$, $g_{\perp} = 1.983$, $A_{\|} = 168 \times 10^{-4}$ cm^{-1} and $A_{\perp} = 64.2 \times 10^{-4}$ cm^{-1}, compatible with a coordination geometry as in **I**. The magnetic susceptibilities of **28** agree with a $V^{IV}O$ formulation for this compound with no antiferromagnetic interactions (see above). The magnetic and spectroscopic results thus suggest the formulation $Na[V^{IV}O(sal\text{-Asp})(H_2O)]$ for compound **28**. However, the elemental analyses, if correct, do not fit this. However, the high carbon and low hydrogen do fit $Na[V^{IV}O(sal\text{-Asp})]$.

From the available results, the formation of a Schiff base complex in solution and in the solid state is clear. The exact structure of **28** remains unclear: in $V^{IV}O(sal\text{-asp})^-$ at least one VO^{2+} coordination position remains free, and only such formulations as $Na_n[V^{IV}O(sal\text{-asp})]_n$ with $n \geq 2$, or $Na_2[V^V_2O_3(sal\text{-asp})_2]$ would be satisfactory. The paramagnetic properties indicate the presence of $V^{IV}O$ ions with independent spins, so formulation as a V(V) complex is incompatible.

3.5.4. Histidine complexes

The elemental analyses for compounds containing histidine are not entirely satisfactory; the solids are probably impure. TLC experiments with samples containing L-His, Hsal and VO^{2+} manifest the complex as a brown spot at $R_f = 0.63$ (**A**) and 0.54 (**B**). If the

mixtures contain 2,2′-bipy, the spots are at $R_f = 0.58$ (**A**) and 0.50 (**B**). In both chromatograms, severe tailing occurs due to decomposition during elution, especially with eluent **B** which contains propionic acid.

From these mixtures, only the solids **29**–**31** are included in Table 1. $\nu_{V=O}$ appears at 970 (**29**), 950 (**30**) and 995 cm^{-1} (**31**). A band at 3140 in **29**–**31** is due to ν_{C-H}(imidazole), the band at ≈ 2600 to ν_{N-H}(imidazole) [36] and at 1470 (**29**), 1495 (**30**) or 1460 cm^{-1} (**31**) to ν_{C-C}(imidazole) [25,36]. The usual bands typical of N-salicylideneamino acidato complexes of oxovanadium(IV) are also present in **29**–**31**. Complexes **29** and **31** have relatively similar IR spectra, but **31** has markedly more intense peaks at 2870 and 2950 cm^{-1} corresponding to aliphatic ν_{C-H} stretch.

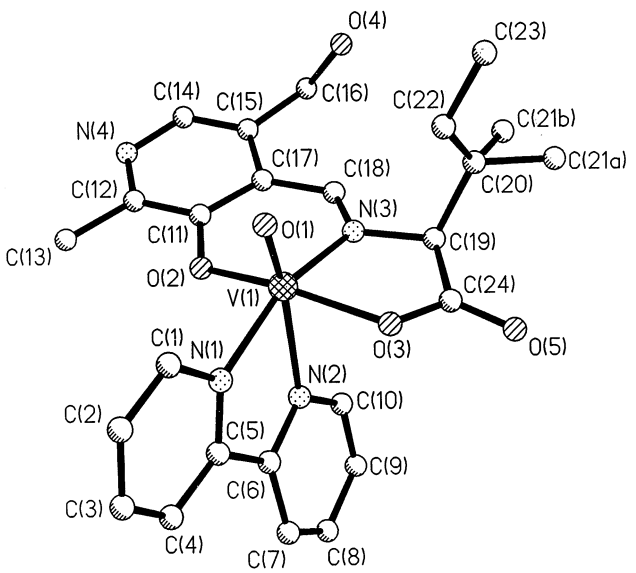

Fig. 5. Diagram of [VO(pyr-D,L-Ile)(2,2′-bipy)]·H_2O (**32**), showing part of the atomic notation. In the molecule shown, isoleucine has configuration L- and vanadium configuration **A** [43].

Table 4
Selected bond distances (Å) and angles (°) for complex **32**

V(1)–O(1)	1.587(9)	V(1)–O(2)	1.939(9)
V(1)–O(3)	2.013(9)	V(1)–N(1)	2.148(10)
V(1)–N(2)	2.332(12)	V(1)–N(3)	2.047(10)
O(3)–C(24)	1.290(14)	C(24)–C(19)	1.510(16)
N(3)–C(19)	1.518(15)	C(19)–C(20)	1.547(18)
N(3)–C(18)	1.301(14)	C(17)–C(18)	1.432(16)
C(11)–C(17)	1.397(15)	O(2)–C(11)	1.333(13)
O(5)–C(24)	1.244(15)		
O(3)–V(1)–N(3)	79.3(4)	O(2)–V(1)–N(3)	87.1(4)
O(2)–V(1)–N(2)	84.4(4)	N(1)–V(1)–N(2)	72.4(4)
V(1)–O(3)–C(24)	118.7(8)	O(3)–C(24)–C(19)	118.7(13)
N(3)–C(18)–C(17)	124.6(12)	V(1)–N(3)–C(19)	115.7(7)
V(1)–N(3)–C(18)	128.2(9)	V(1)–O(2)–C(11)	128.1(9)
C(11)–C(17)–C(18)	120.8(11)	C(18)–N(3)–C(19)	116.1(10)
O(2)–C(11)–C(17)	126.1(13)	N(3)–C(19)–C(24)	106.2(10)

The CD spectrum of **29** dispersed in Nujol mulls is included in Fig. 4. Its pattern resembles that for [V^{IV}O(sal-L-Ala)(H_2O)] [3], indicating a similar coordination geometry. Compound **30** presents no CD signal; possibly here too, racemization of the amino acid was activated by coordination as its Schiff base.

Casella et al. [14] prepared V^{IV}O(sal-L-his)$(H_2O)_2$ denoted here by **C**. Its reported N and H analyses (% N = 11.20, % H = 3.80) were close to those for **29**, but were lower for carbon (% C = 43.45). Reported IR data were identical to our results for **29**. Casella et al. [25] also mention that Hsal and L-His may react slowly forming a cyclic product, and similar reactions occur for pyridoxal [37,38]: the X-ray structure of the Cu(II) complex of one of the intermediate cyclised Schiff bases is known [38]. Several other solids (not described here) were obtained from these mixtures with L-His: their IR spectra were complex, including broad bands perhaps due to oligomeric vanadium compounds.

C, **29** and **30** all have strong bands at 1620 and **31** at 1630 cm^{-1} corresponding to $\nu_{C=N}$. Further, in their CD spectra (UV) **29**–**31** resemble most VO^{2+} Schiff base complexes here: e.g. for **29**: 230 nm ($\Delta\varepsilon = -3.2$ dm^3 mol^{-1} cm^{-1}), 252 nm ($\Delta\varepsilon = +4.1$), 285 nm ($\Delta\varepsilon = -2.5$) and 365 nm ($\Delta\varepsilon = -3.2$, imine band). Complexes **29**–**31** are probably open-chain Schiff base complexes. Whether the imidazole N atom is coordinated axial or not is unclear.

3.6. Pyridoxylideneamino acidato complexes

The brown compound [VO(pyr-D,L-Ile)(2,2′-bipy)]·H_2O where pyr-D,L-ile = N-pyridoxylidene-D,L-isoleucinate was prepared from H_2O/MeOH (or /EtOH) solutions. In other similar preparations with other amino acids and with L-Ile no precipitation normally occurred. When solids formed, their elemental analysis was incompatible with simple formulations.

The structure of **32** was independently solved for two crystals, obtained from different batches, whose final refinement led to $R_1 = 12.31\%$, $s = 1.037$ and $R_1 = 13.14\%$ and $s = 1.82$, respectively. The high R values are due mainly to the poor quality of both crystals. A molecular diagram of **32** is shown in Fig. 5; it exhibits essentially an octahedral geometry and the vanadium atom is 0.319(7) Å from the least squares plane defined by the equatorial atoms O(2), N(3), O(3), N(1) and towards the vanadyl oxygen. Atoms C21A and C21B are disordered with occupancies of 64 and 36%, respectively. Selected bond lengths and angles are given in Table 4.

The pyridoxal ring and all atoms of the chelate rings formed by pyr-D,L-Ile are planar (rms deviation: 0.090). Atom O5 is away from this plane by 0.424(16) Å. The dihedral angle between the directions defined by V(1)–O(1) and C(19)–C(20) is 8.01(1.25)°, the angles between

the directions defined by V(1)–O(1) and C(19)–C(22), and V(1)–O(1) and C(19)–C(20) are 12.7 and 44.2°, respectively. The torsion angles C(20)–C(19)–C(24)–O(3) and C(20)–C(19)–N(3)–V(1) are −108.8 and −112.8° [39,40], respectively, and the angles C(24)–C(19)–C(20) and N(3)–C(19)–C(20) are 109.0(12) and 112.7(12)°, respectively. This means that the side group of the amino acid is roughly parallel to the V=O bond and both the amino acid side group and α-hydrogen atom are out of the plane of the Schiff base.

It was proposed [41,42] that for the key enzyme function, the bond to be broken must be perpendicular to the plane of the extended conjugated system. It is in this conformation that the breaking σ-bond achieves maximal orbital overlap with the π-system of the ligand. At least in the solid state complex **32** has the planarity thought to be essential in facilitating the reactions, except that neither the side group nor the α-hydrogen atom are in the plane. In solution, appropriate electron displacements leading to either removal of the side group (e.g. β-elimination), or the α-hydrogen atom (racemization) are possible. In several N-salicylideneamino acidato oxovanadium(IV) complexes [3,5] the Schiff base ligand is not planar, and this may indicate that such systems are not as efficient in catalysing these reactions.

Besides normal van der Waals interaction, the structure is stabilised by a hydrogen bond network in which each water molecule acts as a double hydrogen donor while N4 and O5 atoms of different molecules act as acceptors: O(W)···O(5) ($x+1$, y, z), 2.844(17) Å and O(W)···N4, 2.859(17) Å [40]. As the vanadium atom is a disymmetric centre, each molecule is a diastereomer containing two disymmetric centres: the two molecules containing L-isoleucine have vanadium with configuration **A**, and in the two containing D-isoleucine vanadium has configuration **C** [43].

Complex [VO(pyr-D,L-ile)(2,2′-bipy)]·H_2O (**32**) has a visible absorption spectrum with broad bands with λ_{max} at 710 and 860 nm, and a high intensity band tailing in from the UV. The EPR spectrum of methanolic solutions of **32** is axial and similar to those observed for several N-salicylideneamino acidato oxovanadium(IV) complexes [3,5]. The spectrum was simulated[2] and the spin-Hamiltonian parameters are: $A_{\|} = 161.9 \times 10^{-4}$ cm^{-1}, $g_{\|} = 1.952$, $A_{\perp} = 56.8 \times 10^{-4}$ cm^{-1} and $g_{\perp} = 1.981$. The $A_{\|}$ and $g_{\|}$ are in the range expected for this type of ligand. Back calculation of $A_{\|}(N_{imine})$ for this complex gives 159×10^{-4} cm^{-1}, in the range of those obtained for [VO(sal-aa)(2,2′-bipy)] N-salicylideneamino acidato complexes [3,5], suggesting electron donation from the N_{imine} to be lower than for most N-salicylideneamino acidato complexes.

[2] See footnote 1.

Acknowledgements

We thank Fundo Europeu para o Desenvolvimento Regional and Fundação para a Ciência e Tecnologia (project: PRAXIS/2/2.1/QUI/151/94) for financial support.

References

[1] F. Bergel, K.R. Harrap, A.M. Scott, J. Chem. Soc. (1962) 1101.
[2] Y. Murakami, H. Kondo, A.E. Martell, J. Am. Chem. Soc. 95 (1973) 7138.
[3] I. Cavaco, J. Costa Pessoa, D. Costa, M.T.L. Duarte, P.M. Matias, R.D. Gillard, J. Chem. Soc., Dalton Trans. (1994) 149.
[4] C. Grüning, H. Schmidt, D. Rehder, Inorg. Chem. Commun. 2 (1999) 57.
[5] I. Cavaco, J. Costa Pessoa, D. Costa, M.T.L. Duarte, R.T. Henriques, P.M. Matias, R.D. Gillard, J. Chem. Soc., Dalton Trans. (1996) 1989.
[6] I. Cavaco, J. Costa Pessoa, D. Costa, M.T.L. Duarte, R.D. Gillard, P.M. Matias, J. Inorg. Biochem. 51 (1993) 157.
[7] S. Dutta, S. Mondal, A. Chakravorty, Polyhedron 14 (1995) 1163.
[8] S. Mondal, S. Dutta, A. Chakravorty, J. Chem. Soc., Dalton Trans. (1995) 1115.
[9] I. Cavaco, J. Costa Pessoa, M.T.L. Duarte, R.D. Gillard, P.M. Matias, J. Chem. Soc., Chem. Commun. (1996) 1365.
[10] R. Hämäläinen, U. Turpeinen, Acta Crystallogr., Sect. C 41 (1985) 1726.
[11] (a) K. Nakajima, M. Kojima, K. Toriumi, K. Saito, J. Fujita, Bull. Chem. Soc. Jpn. (1989) 62. (b) K. Nakajima, M. Kojima, K. Toriumi, K. Saito, J. Fujita, Bull. Chem. Soc. Jpn. (1989) 760.
[12] R. Fulwood, H. Schmidt, D. Rehder, J. Chem. Soc., Chem. Commun. (1995) 1443.
[13] S. Mondal, P. Ghosh, A. Chakravorty, Inorg. Chem. 36 (1997) 59.
[14] L. Casella, M. Gullotti, A. Pintar, S. Colona, A. Manfredi, Inorg. Chim. Acta 144 (1988) 89.
[15] J. Costa Pessoa, J.A.L. Silva, A.L. Vieira, L. Vilas Boas, P. O'Brien, P. Thornton, J. Chem. Soc., Dalton Trans. (1992) 1745.
[16] I. Cavaco, J. Costa Pessoa, S. Luz, M.T.L. Duarte, P.M. Matias, R.T. Henriques, R.D. Gillard, Polyhedron 14 (1995) 429.
[17] L.J. Theriot, G.O. Carlisle, H.J. Hu, J. Inorg. Nucl. Chem. 31 (1969) 2841.
[18] V. Vergopoulos, W. Priebsch, M. Fritzsche, D. Rehder, Inorg. Chem. 32 (1993) 1844.
[19] D.E. Metzler, M. Ikawa, E.E. Snell, J. Am. Chem. Soc. 76 (1954) 648.
[20] J.R. Fisher, E.H. Abbott, J. Am. Chem. Soc. 101 (1979) 2781.
[21] R.P. Houghton, Metal Complexes in Organic Chemistry, Cambridge University Press, Cambridge, 1979, p. 101ff.
[22] A.E. Martell, Acc. Chem. Res. 22 (1989) 115.
[23] E.D. Moffat, R.I. Little, Anal. Chem. 31 (1959) 926.
[24] J.W. Leadbetter Jr., J. Phys. Chem. 81 (1977) 54.
[25] L. Casella, M. Gullotti, J. Am. Chem. Soc. 103 (1981) 6338.
[26] K. Nakamoto, Infrared and Raman Spectra of Inorganic Compounds, 5th ed., 1997, p. 271.
[27] N.D. Chasteen, in: L.J. Berliner, J. Reuben (Eds.), Biological Magnetic Resonance, vol. 3, Plenum, New York, 1981, p. 53.
[28] R. Kuroda, Y. Saito, in: K. Nakanishi, N. Berova, R.W. Woody (Eds.), Circular Dichroism. Principles and Applications, VCH, New York, 1994, pp. 223–225.
[29] L. Casella, M. Gullotti, Inorg. Chem. 25 (1986) 1294.

[30] C.J. Ballhausen, H.B. Gray, Inorg. Chem. 1 (1962) 111.
[31] (a) L. Casella, M. Gullotti, G. Pacchioni, J. Am. Chem. Soc. 104 (1982) 2386. (b) L. Casella, M. Gullotti, A. Pasini, A. Rockenbauer, Inorg. Chem. 18 (1979) 2825. (c) G.N. Weinstein, M.J. O'Connor, R.H. Holm, Inorg. Chem. 9 (1970) 2104. (d) M.R. Wagner, F.A. Walker, Inorg. Chem. 22 (1983) 3021.
[32] J.A. Bonadies, C.J. Carrano, J. Am. Chem. Soc. 103 (1986) 4088.
[33] I. Cavaco, J. Costa Pessoa, in preparation.
[34] S.P. Rath, K.K. Rajak, S. Mondal, A. Chakravorty, J. Chem. Soc., Dalton Trans. (1998) 2097.
[35] S. Mondal, S.P. Rath, K.K. Rajak, A. Chakravorty, Inorg. Chem. 1 (1998) 1713.
[36] C.J. Pouchert, in: C.J. Pouchert (Ed.), The Aldrich Library of Infrared Spectra, 3rd ed., Aldrich Chemical Company, Milwaukee, WI, 1981, p. 1195.
[37] H.M. Dawes, T.N. Waters, J. Chem. Soc., Chem. Commun. (1982) 1390.
[38] K. Aoki, H. Yamazaki, J. Chem. Soc., Chem. Commun. (1984) 410.
[39] G.M. Sheldrick, SHELXS-86, in: G.M. Sheldrick, C. Krüger, R. Goddard (Eds.), Crystallographic Computing 3, Oxford University Press, Oxford, 1986.
[40] G.M. Sheldrick, SHELXL-97, Program for Crystal Structure Refinement, University of Göttingen, Germany, 1997.
[41] H.C. Dunathan, Proc. Natl. Acad. Sci. USA 55 (1966) 712.
[42] J.C. Vederas, H.G. Floss, Acc. Chem. Res. 13 (1980) 455.
[43] G.J. Leigh, in: G.J. Leigh (Ed.), Nomenclature of Inorganic Chemistry, Blackwell, Oxford, 1990, p. 186.